The Influence of Particle Shape on Granular Hopper Flow

Mollon G. [a] and Zhao J. [b]

[a] *3SRLab, UJF-Grenoble 1, Grenoble INP, CNRS UMR 5521, Grenoble F-38041, France*
[b] *Department of Civil and Environmental Engineering, HKUST, Clearwater Bay, Kowloon, Hong Kong*

Abstract. This paper presents a DEM study of the effect of particle shapes on granular flows through hoppers, based on a novel method of generation and packing of realistic sand samples proposed recently by the authors (Mollon and Zhao 2012). Realistic 2D particles of Toyoura sand are used as a demonstrative example. During the flow, we monitor closely the velocity field, the particles rotations, the coordination number, the stress fields and the fabric evolution. These results are compared to the corresponding cases using circular particles. It appears that the use of non-circular particles during the granular flow leads to reduced flow-rate, changes the velocity field towards funnel-flow, localizes particles rotations, increases coordination number, and induces complex behaviors in shear stresses and fabric anisotropy.

Keywords: Discrete modelling, Particle shape, Hopper Flow, Fabric Anisotropy, Dynamic Arching.
PACS: 45.70.Mg, 45.70.Qj

INTRODUCTION

Hopper flows of granular materials are of primary importance in several industrial fields, including mining and pharmaceutical industries, but also have a considerable scientific interest because they exhibit some phenomena which are specific to granular materials. They have thus received great attention from scholars across many communities for decades. More recently, there have been significant progresses towards the comprehension of such phenomena, thanks to the developments of new experimental techniques (e.g. Vivanco et al. 2012) and the availability of advanced computing facilities and numerical tools such as discrete element method (DEM, e.g. Cleary and Sawley 2002).

Mollon and Zhao (2012a) recently proposed a novel method for generating 2D DEM samples of sand with complex but controlled particle shapes (it has been extended to generate 3D particles by the authors, see Mollon and Zhao, 2012b). These shapes are randomly generated based on Fourier spectrums obtained experimentally on sand samples (Das 2007), and packed in a virtual container using a cell-filling methodology based on Voronoi tessellation. To ensure a realistic size distribution of the particles, the Voronoi tessellation is constrained based on a novel algorithm. Finally, each particle shape is filled with several discs of various diameters for further introduction in a DEM code, following the ODEC framework proposed by Ferellec and McDowell (2010). The source code of the program is available for download at *http://guilhem.mollon.free.fr*.

Based on this method, it is now possible to generate 2D samples in an arbitrary geometrical domain and in a rather dense state (when compared to other generation methods), with a prescribed size distribution and prescribed shape features (either with respect to a measured Fourier spectrum or with respect to chosen values of geometrical descriptors such as elongation, circularity, roundness, etc.). This method is employed in the present paper to simulate the flow of sand through a wedge-shaped hopper.

SIMULATIONS

Four simulations (A to D) are performed and analyzed hereafter, each of them involving the flow of roughly 6000 particles through a wedge-shaped hopper with a 60° opening angle. Particles are generated in the container and compacted by gravity, and the flow is triggered by removing the lower face of the hopper. Simulations are performed with ITASCA PFC2D, with a constant interparticle and wall-particle friction coefficient equal to 0.4 and a unit weight of 26.5kN/m². Simulations B and D attempt to simulate Toyoura sand, with realistic average particle diameter (D=0.25mm) and size distribution (C_u=1.24), while simulations A and C deal with circular particles with the same size distribution. The width of the hopper outlet is equal to L=3.75mm (=15D) for simulations A and B, and to L=2.5mm (=10D) for C and D.

The mass discharges over time for the four simulations are plotted in Fig. 1. It is shown that the flow rate of the sand is reduced by roughly 25% in B/D when compared to the circular particles A/C. This ratio is quite similar in the two cases of opening. The non-circular shapes of sand particles indeed cause a rather strong restriction of their kinematics and thus lead to different flow rates for the hopper flow.

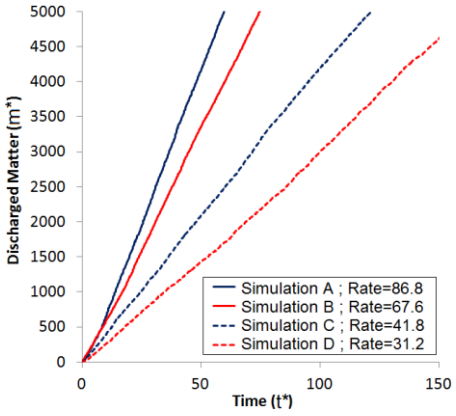

FIGURE 1. Evolutions of the discharged mass (expressed in terms of a normalized mass $m^* = \rho\pi D^2/4$) along time (expressed in terms of a normalized time $t^* = \sqrt{D/g}$), and corresponding flow rates (in terms of m^*/t^*) for the four simulations

POST-PROCESSING

In order to obtain a precise quantification and thence insight of the flows, a specific post-processing method is chosen. A polar mesh is defined to compute the time-averaged fields of several quantities to ignore the flow fluctuations and focus on their persistent characteristics. It is noted however that these fluctuations play an important role in the flow, and will be closely studied in a future paper. The mesh is composed of 621 cells with a rather homogeneous area, each cell containing 5 to 10 particles at a given time. The time-averaging interval is 0.1s, and starts at a time t_1 chosen in order for the mesh to be constantly filled with matter (i.e. the free surface never crosses the mesh).

Every 10^{-4} second (i.e. 1,000 times in the time interval), we consider for each cell of the mesh the relevant particles (i.e. the ones for which the centre is located in the cell), and compute all the relevant local quantities (e.g. average velocity magnitude or mean stress) of this subset. The 1,000 values computed for each cell along the time interval are then averaged, and the resulting average fields are plotted in Figs. 3 and 4.

HOPPER FLOW KINEMATICS

Average fields of the velocity, the angular velocity and the coordination number are provided in Fig. 3 for the four simulations. For a given material, the spatial distribution of the velocity magnitudes seems to be unaffected by the opening width (except that all velocities are roughly divided by two when the opening width is decreased from 15D to 10D). However, the shapes of granular particles have an appreciable influence on the velocity field, since the simulations with sand lead to much narrower flows than the ones with discs, almost tending to a funnel flow.

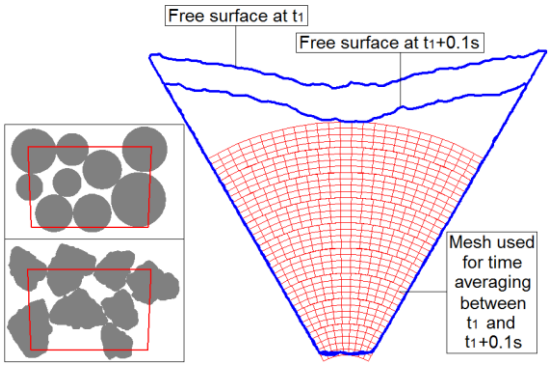

FIGURE 2. Mesh used for time averaging between instants t_1 and t_1+0.1s. The free-surface corresponds to Simulation B. The insert shows typical particles belonging to a given cell

This may be explained by observing the rotational velocity fields. For a given opening width, it appears that the rotational velocities are roughly twice more important in discs than in non-circular particles. For all simulations, very high rotational velocities occur in the lower part of the hopper, due to the change of flow regime at the proximity of the opening. Above this zone of high disturbance, rotations are less intense. In the case of discs, there are considerable particle rotations close to the lateral walls but limited rotations in the bulk. In contrast, in the case of sand grains, particles close to the walls do not rotate much, but we can observe two vertical lines of high rotational velocities which are very well correlated with the contour of the central zone of high velocity magnitude. Non-circularity hence tends to trigger a localization of shearing in the bulk flow, because the rotational contribution to the shearing is restricted on the walls.

The last row of Fig. 3 shows the spatial distribution of the coordination number. Highly non-circular shapes may enhance significantly the number of contacts since multi-contacts between a single pair of particles are allowed in this case. The coordination number is slightly larger than 3 and is rather homogeneous for the simulations with discs. It is closer to 5 or 6 and is not homogeneous for the simulations of sand flow. The coordination number is smaller in the lower part of the flow, and tends to be larger close to the lateral walls. It also appears that the zones of intensified grain rotations correlate quite well with the zones with smaller coordination number. The grain rotations are thus related to loss of contacts and of rotational interlockings between grains.

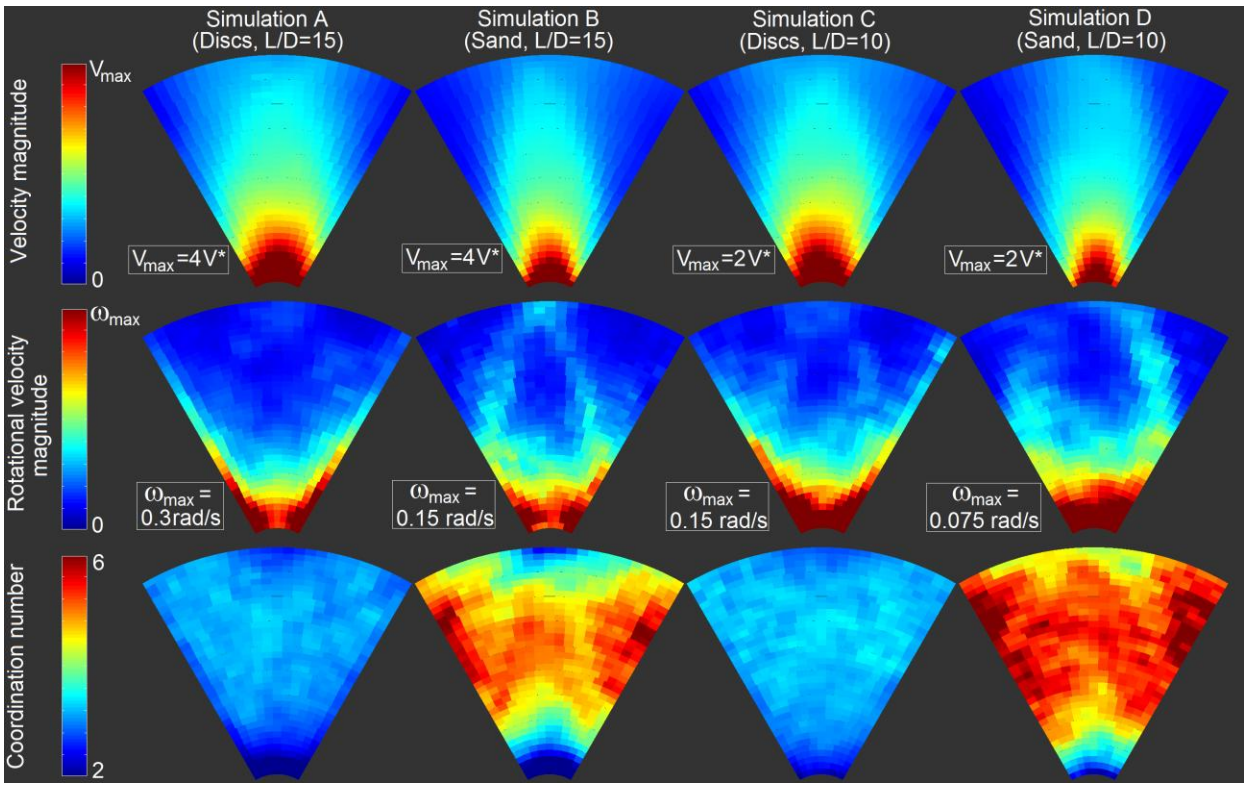

FIGURE 3. Flow kinematics: time-averaged fields of velocity (in terms of a normalized velocity $V^* = \sqrt{gD}$), angular velocity, and coordination number

STRESSES AND FABRIC

The stress and contact fabric fields are plotted in Fig. 4 using the same post-processing algorithm. For all these force-related quantities, it clearly appears that the opening width does not play a major role, since simulations A and C (respectively B and D) lead to very similar results.

For the mean-stress field $(\sigma_1+\sigma_3)/2$, both kinds of granular materials lead to a similar distribution, with low stresses in the lower part (decompression due to the proximity of hopper exit) and in the upper part (less particles weighting above), and stress concentrations in the middle part of the flow, especially at the proximity of the lateral walls. These concentrations are more intense in the case of non-circular particles, and they seem to be located slightly higher on the lateral walls. These high stresses close to the walls are the signature of granular arching.

In the simulations with discs, the shear stress $(\sigma_1-\sigma_3)/2$ remains low everywhere in the flow, while the sand particles lead to obvious high shear stresses located close to the lateral walls. One may conclude that the non-circularity of the particles induces a modification of the arching patterns, allowing the force chains to develop more strongly and to deviate from the purely normal direction. On the macroscopic scale this phenomenon corresponds to an increase of the friction angle.

These observations are further confirmed by the results provided in Fig. 4 in terms of contact fabric anisotropy. This fabric is described by a tensor which depends on two parameters which are described in details in Fu and Dafalias (2012). The contact fabric anisotropy ratio is related to the intensity of the anisotropy of inter-particle contacts (equal to 0 for perfect isotropy and to 1 for perfect anisotropy). The direction of this anisotropy is given by the second parameters, called the contact fabric orientation. The fields plotted in Fig. 4 show that the circular particles do not induce major anisotropy in the contact directions (ratio smaller than 0.1), which means that the anisotropic force chains are not very developed. Comparatively, the sand particles do induce such anisotropy more intensely (ratio closer to 0.4).

The orientation of this contact anisotropy is close to ±45-50° (on the left- and the right-hand side respectively) and remains rather constant on each half of the flow. Since the hopper opening angle is equal to 60°, it means that the non-circularity induces a deviation of the force chains of roughly 15-20° with respect to the direction normal to the lateral walls.

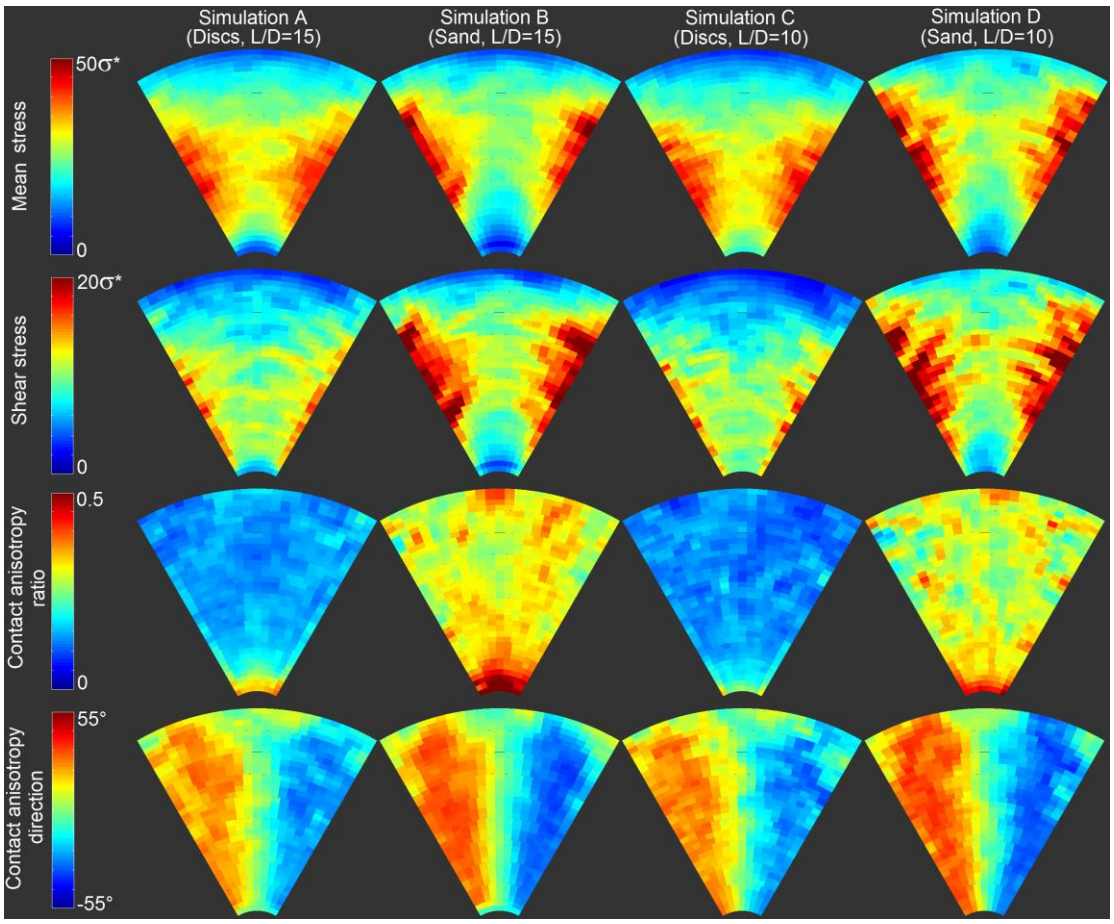

FIGURE 4. Time-averaged fields of mean and shear stress (in terms of a normalized stress $\sigma^* = \pi\rho gD/4$) and of contact-fabric anisotropy ratio and direction

CONCLUSION

The results presented in this paper demonstrate several changes of the behavior of granular hopper flows induced by the non-circular shapes of the particles. Compared to the circular particles case, non-circular particles tend to increase the coordination number and to reduce the rotational velocities during the flow. Rotations are prevented close to the side walls, which leads to the occurrence of localized shear bands of higher rotation in the bulk and a narrower velocity field which tends towards a funnel flow.

It also appears that the non-circularity may totally change the contact patterns, facilitating the development of shear stresses, strong anisotropic force chains and arching. The direction of these force chains is deviated from the normal direction to the walls, showing an increase of the internal friction angle. A close study of the arching patterns (length and life-time of the force chains) will be necessary to understand the micromechanical reasons of this shape-related change of behavior.

REFERENCES

1. G. Mollon and J. Zhao, *Granular Matter* **14**, 621-638 (2012a).
2. F. Vivanco, S. Rica and F. Melo, *Granular Matter* **14**, 563-576 (2012).
3. P.W. Cleary and M.L. Sawley, *Applied Mathematical Modelling* **26**, 89-111 (2002).
4. G. Mollon and J. Zhao, *Granular Matter* In press. doi: 10.1007/s10035-012-0380-x. (2012b).
5. N. Das, "Modeling three-dimensional shape of sand grains using Discrete Element Method", Ph.D. Thesis, University of South Florida, 2007.
6. J.-F. Ferellec and G.R. McDowell, *Granular Matter* **12**, 459-467 (2010).
7. P. Fu and Y.F. Dafalias, *International Journal for Numerical and Analytical Methods in Geomechanics* **35(18)**, 1918-1948 (2011).